544 *Chem. Mater.* **2011,** *23,* 544–553
DOI:10.1021/cm1022344

CHEMISTRY OF MATERIALS
Review

Tailored Organic Electro-optic Materials and Their Hybrid Systems for Device Applications†

Jingdong Luo,‡ Su Huang,‡ Zhengwei Shi,‡ Brent M. Polishak,§ Xing-Hua Zhou,‡ and Alex K−Y. Jen*,‡,§

‡*Department of Materials Science and Engineering and* §*Department of Chemistry, University of Washington, Seattle, Washington 98195, United States*

Received August 6, 2010. Revised Manuscript Received October 18, 2010

Recent development of tailored organic electric-optic (OEO) materials and their applications in hybrid device systems has been reviewed. Hybrid systems encompass the optical and/or electrical components that form intimate contact with OEO materials, such as metal oxide barrier layers, solution processable passive waveguides, silicon nanoslots, and photonic CMOS chips, etc. These systems offer unique advantages combining excellent properties and simple processing for advanced photonic device platforms. Examples include the demonstration of low-V_π and low-loss EO modulators in hybrid polymer sol−gel waveguides, CMOS-compatible hybrid polymer/silicon slotted waveguides, and EO polymer-clad silicon nitride ring resonator modulators. This review also provides a future prospect for the development of OEO materials and their hybrid systems.

1. Introduction

Organic electro-optic (OEO) materials and their hybrid systems have received considerable attention for a variety of emerging photonic technologies.[1−3] OEO materials are based on the linear EO effect (or Pockels effect) which quantifies how the refractive index (Δn) of such materials varies proportionally with the applied electric field strength (E) according to the equation of $\Delta n = n^3 rE/2$, where r is the material's EO coefficient. Thus, an electrical signal can be used to control the amplitude, phase, frequency, or direction of the light beam within the EO material, leading to one of the most widely used mechanisms for high-speed optical modulation and sensing devices. The ideal materials for EO applications need to simultaneously possess a large EO coefficient, excellent thermal stability, high optical transparency and power handling capability, and low dielectric constant. Ideally, these hybrid systems of OEO materials will be able to combine excellent EO properties with simple processing to achieve exceptional performance in a variety of high-speed optical modulation and sensing devices.

This short review focuses mainly on the recent development of tailored OEO materials and their hybrid systems for device applications. The coverage of OEO materials includes dipolar chromophores and their poled polymer and dendrimer systems, which exhibit both large EO activity and processing adaptability for integrated photonics. The hybrid systems include the optical and/or electrical components that form intimate contact with OEO materials, such as the barrier layers, solution-processable passive waveguides, silicon nanoslots and photonic CMOS chips, etc. These systems are devised with unique advantages to the ultimate implementation of highly efficient OEO materials, and the role of interfaces between organic, metal oxides, and metal could be predominant. The readers of this article can refer to a number of excellent reviews, feature articles, and book series that have been devoted to the earlier development and more general survey of organic second-order nonlinear optical (NLO) materials.[4]

Section II covers the approach of enhancing Pockels coefficient (r_{33} value) in poled EO polymers with a layer of spin-on bottom clad, the systematic study of the electrical conduction mechanisms of highly efficient EO polymers during high-electric-field poling, followed by the latest progress in the development of low-drive-voltage polymer sol−gel modulators with low insertion loss.

In section III, the research progress and challenges faced in EO polymer/silicon hybrid systems are summarized. By using simple guest−host EO polymers with in-device r_{33} values of less than 40 pm/V, such systems have already been shown to have superior performance (such as the demonstration of a halfway voltage of 0.25 V EO modulator) compared to those achieved in either silicon or polymer individually. A record-high r_{33} values of 735 pm/V at 1550 nm has also been achieved in EO polymer infiltrated photonic crystal slot waveguide modulators through the slow light effect. This represents more than one order enhancement of r_{33} value compared to the EO activity of thin film/ITO device using the same material. The performance of these devices is expected to be further enhanced if higher r_{33} OEO materials can be integrated into optimized silicon nanoslotted waveguides.

Section IV is devoted to the research in OEO materials as a valid near-term solution to chip-to-chip optical interconnects for tera-scale computing. A very effective molecular

† Accepted as part of the "Special Issue on π-Functional Materials".
*Corresponding author. E-mail: ajen@u.washington.edu.

 Published on Web 11/04/2010

engineering approach for providing reinforced site isolation of highly polarizable dipolar chromophores has also been developed to increase thermal stability of poled polymers/dendrimers for high temperature on-chip applications.

This review is concluded with a prospect outlook to the future development of OEO materials and their hybrid systems.

2. Enhancement of Pockels Coefficient for Poled Polymers in Multilayered Structures

The polar order in EO polymers could be achieved by applying high electric field to align the chromophore dipoles while the film is heated to the glass-transition temperature (T_g).[4,5] This process is commonly used in poling single-layer EO films to allow convenient characterization of NLO properties and screening of materials. Usually, the maximum EO coefficient for a given polymer is achieved at the highest applicable poling field, often to a level where it nearly generates dielectric breakdown. Such high fields could induce local electrical discharges in low-density domains of the material, and lead to high leak through currents (LTC) that can cause physical damages to the poled films. Therefore, considerable research efforts have been spent on improving high field poling of EO polymers. Most of these studies are guided by using the knowledge learned from research in the high field conduction and breakdown of insulating polymers.

One effective approach to improve the poling of EO polymers is to insert a thin layer of spin-on materials as a barrier between the electrode and the EO layer to form a double-layer structure between the two poling electrodes (Figure 1). By careful selection of barrier material, this additional layer can be used to effectively block the excessive LTC and suppress the onset of catastrophic breakdown to enhance the maximum applicable poling field. This provides ample insight to the electrical conduction phenomena of EO polymers. For waveguide device applications, the selection of suitable cladding materials is very critical to the efficiency of device fabrication and operation. Therefore, the intensive study of suitable clad has also led to recent rapid development of low modulation voltage (V_π) and low insertion loss hybrid polymer sol−gel EO modulators.

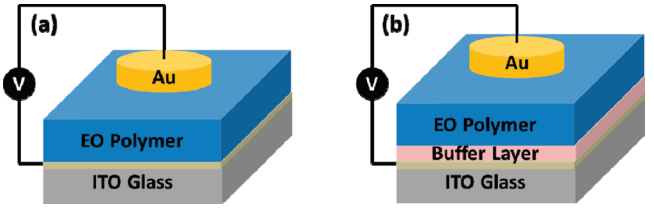

Figure 1. Sandwiched (a) single-layer and (b) double-layer structures for the poling of thin film OEO materials.

Eich et al. have reported the first comprehensive study on high-electric-field poling of side-chain poly(methyl methacrylate-co-Disperse Red 1 methacrylate) (PMMA/DR1).[5] They have investigated the electrical conduction phenomena during the poling of PMMA/DR1, and found that the current densities appeared to be interface (electrode) limited. The electric current and second-harmonic measurements were performed simultaneously to derive the effective internal field strength. As shown in Figure 2, the field dependence of the current density was primarily dependent on Schottky emission for medium field strengths ($E_{pol} \leq 100$ V/μm), whereas it was dominated by Fowler−Nordheim tunneling at higher poling fields. By introducing a spin-on inorganic siloxane barrier layer, the tunneling currents were significantly suppressed and the probability of dielectric breakdown was greatly reduced, leading to 20% higher effective internal poling field strength and higher degree of orientational order of poled films.

Following the aforementioned study, Drummond et al. have used a conductive-polymer-based cladding layer to enhance the poling in guest−host PMMA/DR1.[6] This study has elucidated how the more conductive cladding layer can improve the poling efficiency of multiple layer films. In conventional optical waveguide devices, the active EO layer needs to be sandwiched between two low-refractive-index cladding layers that have similar thickness to the active EO layer. During poling, this triple-layer stack can be simply treated as three resistors in series, and higher conductivity cladding layers can lead to more effective poling field across the active layer. Recently, researchers have also used the blend of a conducting polymer, poly (ethylene dioxythiophene) (PEDOT):

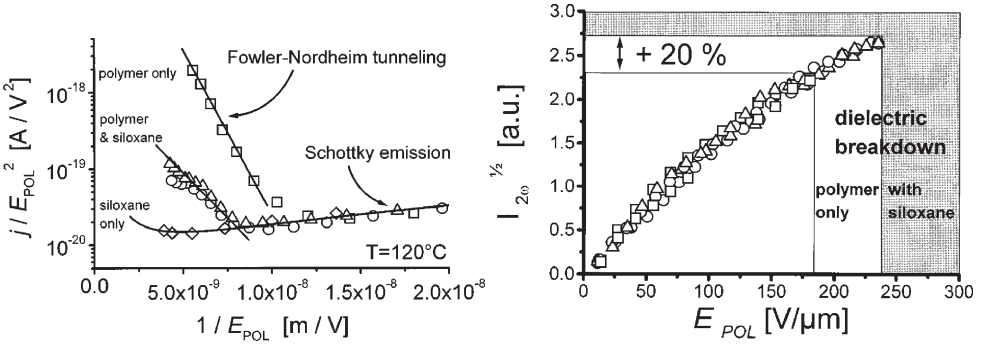

Figure 2. Left: Fowler−Nordheim diagram, i.e., (j/E^2) vs $1/E$ for PMMA/DR1 films with or without additional siloxane layers. Squares, polymer only; circles, polymer with 0.13 μm siloxane layer; triangles, polymer with 1.1 μm siloxane layer; Diamonds: single inorganic layer. Right: Square root of second harmonic intensity that is proportional to the achieved degree of chromophore orientation as a function of the applied electric field across the NLO layer defined as $E_{POL} = U_{POL}/d_{TOTAL}$. Figure reproduced with permission from ref 5b. Copyright 1998 Optical Society of America.

poly (styrene sulfonate) (PSS) with poly (vinyl alcohol) (PVA) as a conductive cladding layer. An effective poling field of 230 V/μm can be applied on the samples with these clad, whereas the best single-layer EO polymer samples can only sustain 160 V/μm. This led to a 15% enhancement of EO coefficient over that of the single-layer control sample, which was mainly attributed to the delayed onset of catastrophic breakdown in the double-layer structures.

Grote et al.[7] have also conducted a thorough analysis of achieving efficient poling and low driven voltage:(V_π) of EO polymers. Prior to this study, the dielectric constants of both the NLO polymer core, such as PMMA/DR1 and amorphous polycarbonate (APC) doped with CLD1 chromophore, and passive polymer cladding materials used for conventional polymer-based integrated optic devices were very similar in magnitude. This suggests that only a small fraction of the applied modulation voltage can reach the NLO polymer core layer. This contributes to 4−5 times higher modulation voltage than the desired V_π. In Grote's study, a 2-fold decrease in modulation voltage could be achieved by using the conductive polymer PEDOT/PSS, due to its much higher conductivity and dielectric constant than the core material at the modulation frequency.

More recently, Norwood and Peyghambarian et al. have reported efficient poling of EO polymers using a modified sol−gel cladding layer, which resulted in a 2.5 times enhancement of r_{33}.[8] The sol−gel cladding is consist of a 95/5 molar ratio of 3-(trimethoxysilyl)propyl methacrylate to zirconium(IV)-*n*-propoxide to provide suitable index, conductivity, and dielectric constant. In addition, more efficient EO polymers, such as guest−host AJL8 and AJLS102 in amorphous polycarbonate, were used for demonstrating low-voltage hybrid polymer sol−gel EO modulators.

After processing, the volume conductivity of sol−gel layer under the poling condition was larger than that of EO core layer by several orders of magnitude, allowing efficient poling of bilayered structures. At the same time, the sol−gel layer has a higher RF dielectric constant compared to the EO core (5 and ~3.5, respectively) at the modulation frequency to secure good modulation efficiency. Moreover, it also provides other benefits such as tunable refractive index, low optical loss, and the capability to be directly patterned with ultraviolet lithography, which makes it more desirable than PEDOT/PSS-based cladding materials.

The current−voltage response of the EO layer with and without cladding was found to follow the model of Schottky−Richardson thermionic emission across a barrier, while the conduction mechanism of the cladding alone follows the trap free space charge limited conduction. This comparison states the different nature of charge transport in EO polymers and sol−gels. This poling technique has resulted in a 2.5 times enhancement of EO coefficient, which is probably the largest improvement observed in poling hybrid polymer/sol−gel films. The r_{33} value of one the guest−host polymer (JT-1) used has

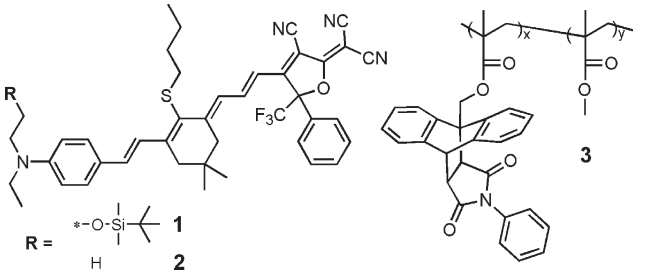

Figure 3. Chemical structures of chromophores and host polymer used in the study of TiO_2-modified transparent electrode for poling. Figure reproduced with permission from ref 12. Copyright 2010 American Institute of Physics.

shown an enhancement from 26 pm/V (when poled as the single layer film) to 65 pm/V using a sol−gel cladding. The enhancement is nearly proportional to the increased dielectric breakdown voltage of the polymer/sol−gel films. It is hypothesized that a space charge layer accumulates at the sol−gel/EO polymer interface, which in general follows approximately the Maxwell−Wagner treatment of multilayered dielectrics.[9] Such charge accumulation inhibits avalanche electron conduction in the EO polymer film, thereby suppressing dielectric breakdown during high field poling.

By incorporating the higher r_{33} EO materials recently developed by Jen et al., the hybrid polymer/sol−gel waveguides have been integrated to demonstrate very low V_π and low-loss EO modulators.[9a] Such hybrid systems include the AJ309/sol−gel waveguide EO modulators which exhibited a record-high in-device r_{33} value of 170 pm/V at 1550 nm and sub-1 V driven voltage,[1a,10] and the strip-loaded AJLS102-APC/sol−gel waveguide with a V_π of 2.8 V and low insertion loss to 5.7 dB.[11]

Very recently, Huang and Jen et al. reported the study on high field poling of EO polymers using a sol−gel-derived ultrathin (40 nm) TiO_2 barrier layer.[12] This research was motivated by new material characteristics associated with highly efficient EO polymers. The EO materials used in this work are AJ-CKL1(**1**)/APC, AJ307, and AJ404 (Figure 3).[13] These material systems usually contain high loading density (N of up to $2.5-3.5\times10^{20}$/cm^3) of large dipole moment tetraene chromophores with strong dialkylaminophenyl donor and CF_3-TCF acceptor, and the HOMO level of such chromophores are around −5.0 eV with the optical band gaps usually around 1.1 eV. When poled at a sandwiched structure of ITO/EO/Au, these polymers show relatively high LTC (and therefore have high DC conductivities around 1×10^{-8} to 1×10^{-11} S/cm) and limited dielectric strength. Such high level of conductivity is several orders higher than that of PMMA/DR1, because of the reduced contact barrier height (BH) of <0.3 eV at the electrode/organic interface as well as much smaller band gaps (i.e., 1.1 eV for AJ-CKL1vs 1.8 eV for DR1).

A TiO_2 layer can be used as an excellent barrier since the BH is around 3.0 eV at the ITO/TiO_2 interface to block excessive hole injection due to its low-lying valence band (~7.4 eV).[14] By utilizing the TiO_2 barrier, the density of LTC was significantly reduced by one to 2 orders

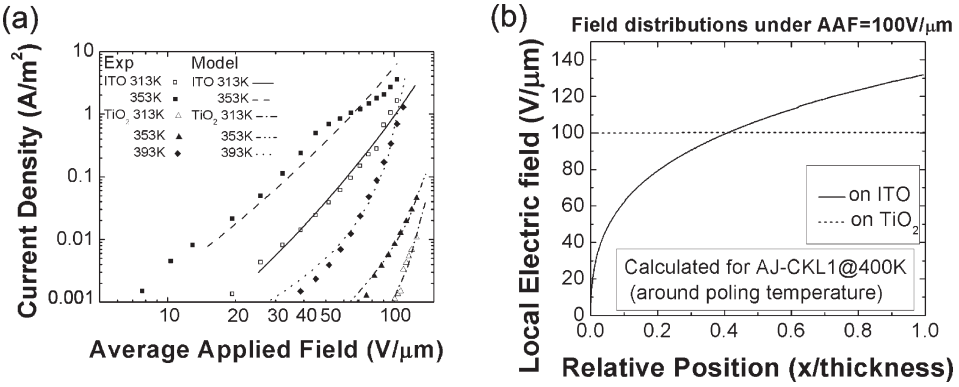

Figure 4. (a) AJ-CKL1 $J-F$ response with/without TiO_2 layer at different temperatures. The dots are experiment results and the lines are from calculation. (b) Using the same parameter from panel a, the field distributions are calculated in a normalized scale. Figure reproduced with permission from ref 12. Copyright 2010 American Institute of Physics.

of magnitude, and ultralarge EO coefficients (up to 160−350 pm/V at 1310 nm) could be achieved. The efficiency of dipole alignment in these poled films was quantified by a series of comparative experiments until the optimal average applied field (AAF) with highest achievable r_{33} values was reached. Plots of r_{33}-AAF show a significant increase in slope by inserting the TiO_2 barrier film compared to the single-layer devices. In the guest−host AJ-CKL1/APC system, the r_{33}-AAF slope increases by 11%, and the extra r_{33} enhancement is mainly due to the elevated poling field strength. In other more active systems with higher chromophore loading (AJ307 and binary EO polymer AJ404), the r_{33} improvements are mainly from the result of steeper r_{33}-AAF slope, which are enhanced by 26 and 40%, respectively. Such enhancement has never been reported from prior studies where the higher r_{33} values of poled films were mainly due to increased poling field, whereas the r_{33}-AAF slopes were nearly unchanged.

These encouraging results have led to more detailed study of conduction mechanisms by measuring the current−voltage ($J-V$) response of EO polymers. The experimental results were compared with a unified model of space charge limited current (SCLC) and injection limited current (ILC). Bässler et al. have first reported this model for studying organic semiconductor devices.[15] It assumes that the conduction mechanism involves a two-step injection process and a hopping SCLC in organic materials with a Gaussian density of states distribution. As shown in Figure 4, the good agreement between the experimental results and calculated values indicates that this analytical model can be applicable to the poling of EO polymers, and the current behavior and field distribution under high poling field can be estimated. The field distribution flattening effects could be the major factor in enhancing the poling efficiency of these EO polymers. This effect can be achieved by using the sol−gel-derived TiO_2 as the barrier layer, which effectively blocks hole injection from the anode and ensures injection remains the rate-controlling factor during poling.[12]

3. Hybrid OEO Silicon Slotted Waveguides

As discussed earlier, the performance of polymer-based EO modulators using low-refractive-index buffer layer have almost reached the same level as commercial $LiNbO_3$-based modulators. By employing suitable nanotechnology tools like e-beam lithography, EO modulators can be made and integrated onto a silicon platform for high degree integration in silicon photonics.[2,3] Silicon photonics are expected to become the key technology for highly integrated optics due to its compatibility with electronics and the mature manufacturing infrastructure of silicon. The past several years have witnessed the rapid growth in the research of silicon photonics. However, the Pockels effect does not exist in silicon because of its centrosymmetric crystal lattice. Therefore, a high-speed, efficient polymer/silicon hybrid modulator requiring a low driven voltage and a small footprint is highly desired.

In hybrid polymer silicon systems, all passive components are fabricated in silicon to form nanoscale slotted waveguides typically with the rail width of <350 nm. Because of the very high refractive index of silicon ($n \approx 3.48$), a large fraction of the guided mode can be concentrated into the low refractive index gap within the center of silicon waveguide, and the optical nonlinearity can therefore be introduced by filling the gap with OEO materials.[2,3] Solution or melt processable organic materials have been identified as the ideal material systems to be infiltrated into various silicon nanostructures.

The first slotted silicon waveguide modulator with OEO materials as clad was reported by Hochberg and Scherer et al.[16] The device consisted of a ring resonator with a radii of 40 μm and a slot width of 140 nm. The YLD124/APC guest−host polymer or a three-arm dendrimer was used as the EO material clad. The experimental results clearly demonstrated that low voltage EO tuning and modulation could be achieved, although the devices were not optimized as high-Q ring resonator modulators. By utilizing the triarm EO dendrimer, the ring-based modulators in this study exhibited tuning up to 5.2 GHz/V, which is about five times more responsive than other modulators designed with similar materials on a nonslotted architecture. However, there are some concerns about the optical loss of the polymers and dendrimers that may be a limiting factor for the higher-Q devices.

Recently, the same group has reported an improved EO polymer-clad silicon slot waveguide modulator using a

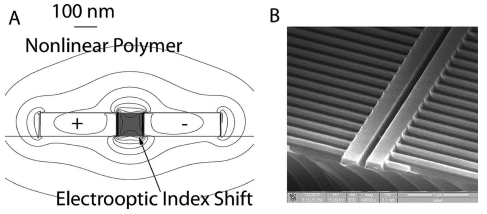

Figure 5. (A) Diagram of the silicon slot waveguide as used in low V_π Mach−Zehnder modulator. The modal pattern near 1550 nm is plotted; contours of $|E|$ are shown. (B) SEM micrograph of a slot waveguide, in this case being coupled to a ridge waveguide. Figure reproduced with permission from ref 17. Copyright 2008 American Institute of Physics.

Mach−Zehnder (MZ) device configuration.[17] In this work, a segmented slot waveguide consisted of two ridges of silicon, narrowly separated from each other by a trench. Figure 5 shows the slot waveguide used for the MZ modulator, with the mode pattern plotted, as well as a scanning electron microscope (SEM) micrograph of a part of a device. The two 300 nm × 100 nm arms are separated by a 120 nm slot, and the MZ arm length is 2.0 cm. The device was poled at 150 V/μm and operated at the push−pull mode. As a result, a half wave voltage of 0.25 V or $V_\pi L$ figure of merit as 0.5 V cm was achieved near 1550 nm. This is one of the lowest values for any modulator obtained to date. Nevertheless, the in-device r_{33} value achieved in polymer YLD124/APC was calculated to be ~30 pm/V. This is much lower than its optimal r_{33} value in sandwiched micrometer thick films. It is very likely that the EO polymer in the slot was not optimally poled.

Another novel concept of making compact hybrid EO modulators is based on the use of photonic crystal resonator structures. These devices are fabricated in a two-dimensional photonic crystal configuration with silicon as core and a nonlinear optical polymer infiltrated as clad. Wülbern and Eich et al. have recently demonstrated that EO modulation in such slotted photonic crystal heterostructures could be achieved by using the guest−host EO polymer AJ-CKL1/APC.[18] The device geometry is ultracompact on the micrometer scale, and extremely sensitive to the refractive index changes in the slot region for ultrafast EO modulation. The index change of the polymer in the 150-nm wide slot was calculated to be approximately $\Delta n = 1.3 \times 10^{-4}$ at 1 V applied modulation voltage; hence, the in-device Pockels coefficient of the EO polymer in this experiment was ~9 pm/V by the poling field of 130 V/μm.

This value is almost one order lower than the value reported in single-layer device using the same material. Lately, using this new device platform, the same group has also demonstrated very high speed EO modulation up to 40 GHz.[19] The modulation frequency was limited only by the available RF source and power feeding scheme. Up to 40 GHz, no significant roll-off in the modulation signal amplitude was observed. This encouraging result indicates that this kind of devices can potentially be operated at even higher bandwidths because the EO effect is based on the pure π-electronic polarization of NLO chromophores.

Chen et al. have also reported a newly designed Mach−Zehnder modulator based on EO polymer (AJ-CKL1/PMMA or AJ-CKL1/APC) infiltrated photonic crystal slot waveguide.[20] This modulator design combines the advantage of excellent optical confinement in silicon slot waveguide, enhancement of r_{33} because of the slow light effect in photonic crystal waveguide, and strong electro-optic response in EO polymers. Through this design, EO modulation can be achieved in a very short active region (352 μm). By matching the mode profile and group velocity between strip and photonic crystal slot waveguide, it enables coupling into slow light regime. The modulator shows a 13 V switching voltage and an improved in-device EO coefficient of 132 pm/V that has been enhanced because of the slow light effect.

More recently, Wang and Chen further optimized their design and fabricated a 320-nm slot for EO polymer infiltrated silicon photonic crystal waveguide.[21] The principle is based on the fact that wider slot waveguide could significantly reduce leakage current, and thus enhanced the poling efficiency. It also greatly relaxes the stringent requirements on device fabrication using e-beam lithography and reactive ion etching. The leakage current during the poling process is monitored *in situ* as shown for the 75 and 320 nm photonic crystal slot waveguide. The peak current density for the 75 nm slot is 575 A/m^2, whereas it is only 7.9 A/m^2 for the 320 nm slot.

Compared to the typical 1−10 A/m^2 leakage current observed during the poling of AJ-CKL1/APC-based thin film device, the poling of the same material in the 320 nm wide slot waveguide shows almost identical poling behavior. A record-high in-device r_{33} value of 735 pm/V and 0.44 V mm $V_\pi L$ product have been achieved. Compared with the r_{33} value of around 75 pm/V at 1.55 μm usually obtained for poling the AJ-CKL1/APC thin film device, the effective in-device EO coefficient is enhanced by almost one order because of the slow light effect of photonic crystals. This exceptional performance is also attributed to the increased poling efficiency of the EO polymer within the 320 nm slot.

Hochberg and Jen et al. have recently demonstrated the high modulation speed in the gigahertz regime in a silicon slot waveguide modulator with EO polymer as clad.[22] The $V_\pi L$ figure-of-merit (FOM) for this modulator is 0.8 V cm, which is within a factor of 2 of the lowest V_π (0.25 V) that was reported.[17] This result demonstrates that the low drive voltages previously achieved in slower speed devices can also be improved to higher speed for RF bandwidth applications. The EO polymer used in this study is based on the guest−host AJSP100 that exhibits a relatively large EO activity (r_{33} value of 65 pm/V at 1550 nm) at a relatively low chromophore loading level of $\sim 1.0 \times 10^{20}$/cm^3, low optical loss (~1 dB/cm at 1550 nm), and good temporal and photochemical stability. The FOM of 0.8 V cm $V_\pi L$ suggested that an in-slot r_{33} of 40 pm/V has been achieved, which is almost 60% of the highest achievable value in the thin film device form. The 3 GHz bandwidth observed was lower than the originally predicted value; however, further design and process optimization should increase the bandwidth of such devices significantly.

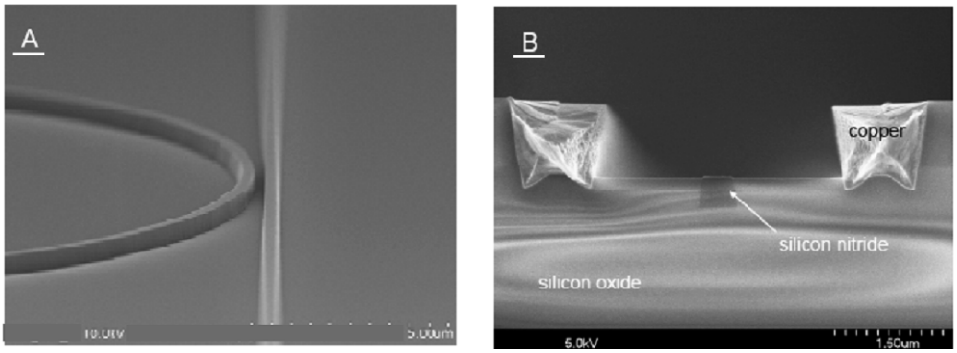

Figure 6. (A) SEM image of a silicon nitride ring resonator after patterning. (B) SEM cross-section of part of the EOP cladding modulator prior to EOP film deposition. Figure reproduced with permission from ref 26. Copyright 2008 Optical Society of America.

One of the main challenges associated with the processing of hybrid OEO silicon slot waveguides is the low poling efficiency of OEO materials in the nanoslot waveguides. Despite numerous attempts there are no appreciable r_{33} values that can be achieved in slots with the newly developed OEO materials (r_{33} values up to 350 pm/V). This result shows that the performance of the devices can be significantly if the poling efficiency in the slot can be enhanced. Although AJSP100 EO polymer has been specifically formulated to give improved electrical properties and better poling efficiency in slot waveguides,[21] further optimization of OEO material is needed. Future studies should focus on understanding the underlying physics of high field poling of OEO materials in submicrometer silicon cavities.[18]

The poling problem in silicon nanoslotted waveguides shows the importance of applying the unified Bässler's model to systematically analyze the conduction mechanism of amorphous organic dielectrics,[15] in which the temperature, field, and thickness dependences of ILC and SCLC of highly efficient OEO materials can be quantitatively described.[23] During the poling of EO polymers, the significant change of leakage currents as a function of slot width deserves further investigation.[21] In particular, the device dimension, surface roughness, and the silicon/polymer interface are three of the key parameters in affecting the materials' conduction mechanism under the poling condition and ultimately determining the device efficiency of various hybrid nanoscale photonic devices.

To reduce the surface roughness of slot waveguides, recently Alasaarela and Säynätjoki et al. have reported the application of a conformal amorphous TiO_2 film that can be easily grown into slot structures using the atomic layer deposition technique.[24] The results from simulations show that a silicon slot waveguide covered with a high refractive index material such as TiO_2 has good electric field confinement in the remaining air slot. The effect of angled sidewalls on the filling and properties of silicon slot waveguides has also been discussed using different oxides and organic materials. This study suggests the possibility of inserting an ultrathin oxide layer, as being demonstrated in sandwiched structure of ITO/TiO_2/OEO/Au,[12] be applicable to improve the poling and device performance of hybrid OEO silicon slot waveguides.

4. Reinforced Site Isolation of OEO Materials for High-Temperature On-Chip Applications

Dramatically increasing data rates require much higher chip-to-chip bandwidth between microprocessors, such as CPU-to-memory and CPU-to-CPU, to minimize the data communication delay. It is envisioned that the CPU-to-memory bandwidth soon will reach 100 GB/s in coming years, and will be further enhanced to the era of tera-scale (tetrabits per second) computing.[25] To reach this scale, traditional electrical interconnects require complicated circuit design, miniaturization of the components, and utilization of more costly materials, which is technically challenging and impractical from the cost and energy consumption points of view. Optical interconnect technology could be an effective solution for this challenge. In the past, various arguments for introducing optical interconnections to silicon CMOS chips have been proposed, and the challenges for optical, optoelectronic, and integration technologies have been discussed.

Recently, the researchers from Intel have demonstrated an innovative concept of "photonics on top of the CMOS" through the direct fabrication of a monolithic optical switching layer on top of the existing CMOS chip without sacrificing original transistor performance.[26] This is another very appealing example of hybrid systems that incorporate highly efficient OEO materials. In this prototype device, the new optical layer can provide an additional mechanism to improve the communication rates between microprocessors. Figure 6 shows the waveguide structure of this prototype device. The EO polymer is selected as a top cladding material for higher index contrast waveguide systems to give more compact devices and closer electrode spacing. The core waveguide in the modulator is 450 nm thick silicon nitride ($n = 2$). The linear EO effect is used to modify the index of EO polymer which modifies the optical mode effective index and imparts an index change that modulates the intensity of light. With this system, ring resonators as small as 21 μm in radius with electrodes spaced at 3 μm can be fabricated, which is considerably smaller than previously reported ring resonator modulator based on an EO polymer waveguide with a 300 μm radius.

By implementing a typical guest−host EO polymer (AJTB141/APC) in the ring resonator modulator, a high

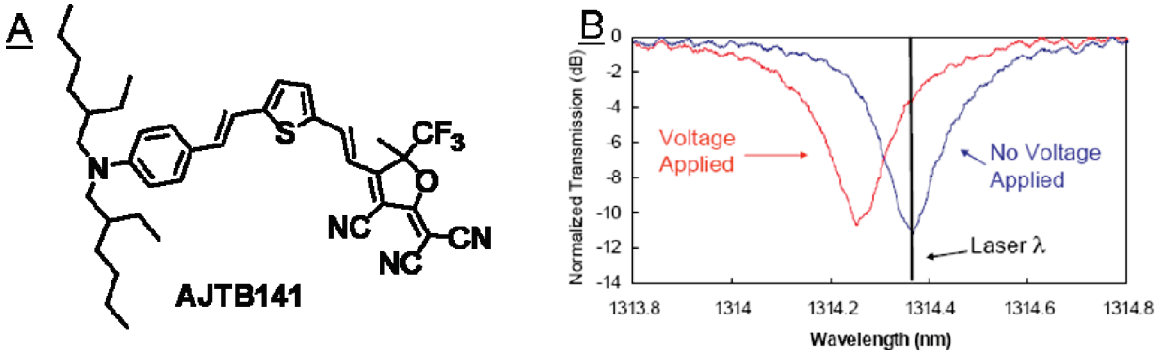

Figure 7. (A) Chemical structure of AJTB141 chromophore; (B) resonator spectra obtained on the EO modulator. Figure reproduced with permission from ref 26. Copyright 2008 Optical Society of America.

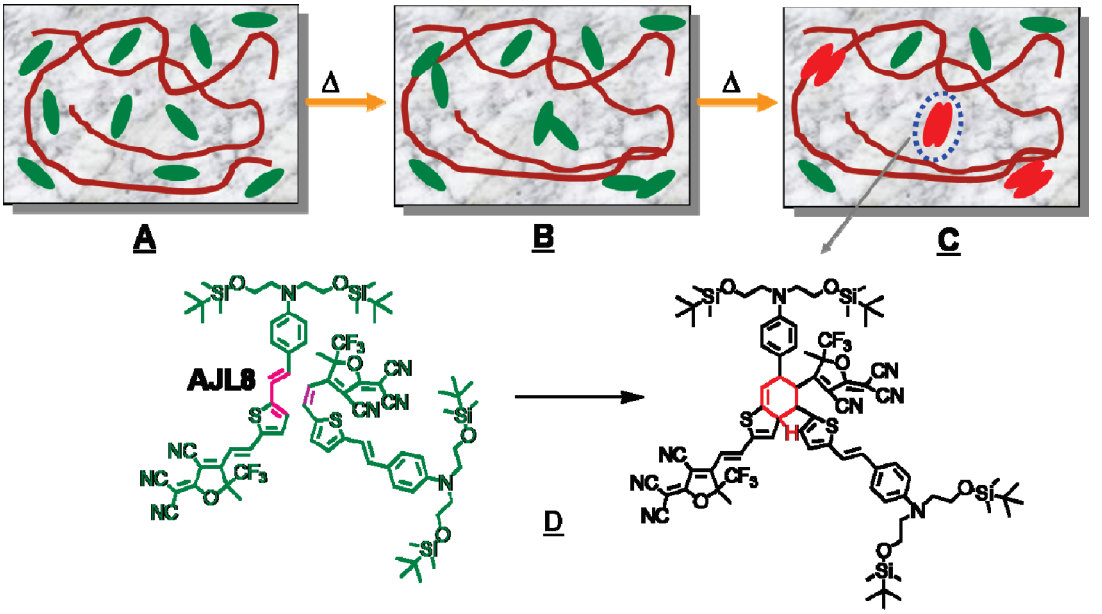

Figure 8. (A−C) Schematic illustration of chromophore decomposition at elevated temperatures (D) and its major decomposition path way.

frequency modulator with modulation observed at 10 GHz and low drive voltage of 2.7 V_{pp} has been demonstrated. The shift of resonance peak was found to be 3 pm/V (Figure 7), which corresponds to an effective in-device EO coefficient around 30 pm/V.[26] Recently, by incorporating more efficient EO polymers into devices, the resonance shift of such device was improved to ~25 pm/V, which can be translated into very large in-device EO coefficient of ~200 pm/V.[27] This result shows that EO polymer clad ring resonator modulators are probably the near-term solution of active components for high-speed chip-to-chip optical interconnects.

The main obstacle for implementing the photo-CMOS device is that the poled devices need to withstand high manufacturing temperatures (up to 300 °C) through the back-end process. In particular, both the chemical composition and poling-induced acentric order of EO lattices need to be stable at elevated temperatures (85−100 °C) and survive a short temperature excursion (30 min at 300 °C).

There are significant advancements in improving the temporal stability of OEO materials at 85 °C to ensure devices can function properly for years.[28] In contrast, there is only limited information about how OEO materials can possess both large r_{33} values and high stability at temperatures greater than 200 °C. Although high-T_g EO polymers, such as side-chain polyimides and polyquinolines, have been explored extensively for high-temperature applications,[29] EO activities of these polymers are very limited, less than 25 pm/V at telecommunication wavelengths, mainly due to the limitation of early generation NLO chromophores, which have low $\mu\beta$ values.

To address the challenge for high-temperature stability in OEO materials, Shi and Jen et al. have systematically investigated the underlying thermal decomposition mechanism and cross-linking conditions of highly efficient OEO materials.[30] The decomposition pathways of new generation highly polarizable NLO chromophores (such as AJL8 and AJLS102) have been identified. As illustrated in Figure 8, chromophore AJL8 contains a styryl thiophene bridge substituted with a strong dialkylaminophenyl donor and a CF_3-TCF acceptor, and there are several potential mechanisms that could lead to chromophore degradation under elevated temperatures. Out of several possible reaction mechanisms, a scheme of bimolecular tandem Diels−Alder (DA) and retro-DA reactions was suggested to be the dominant decomposition pathway of AJL8. Initially, when doped into a host polymer, these

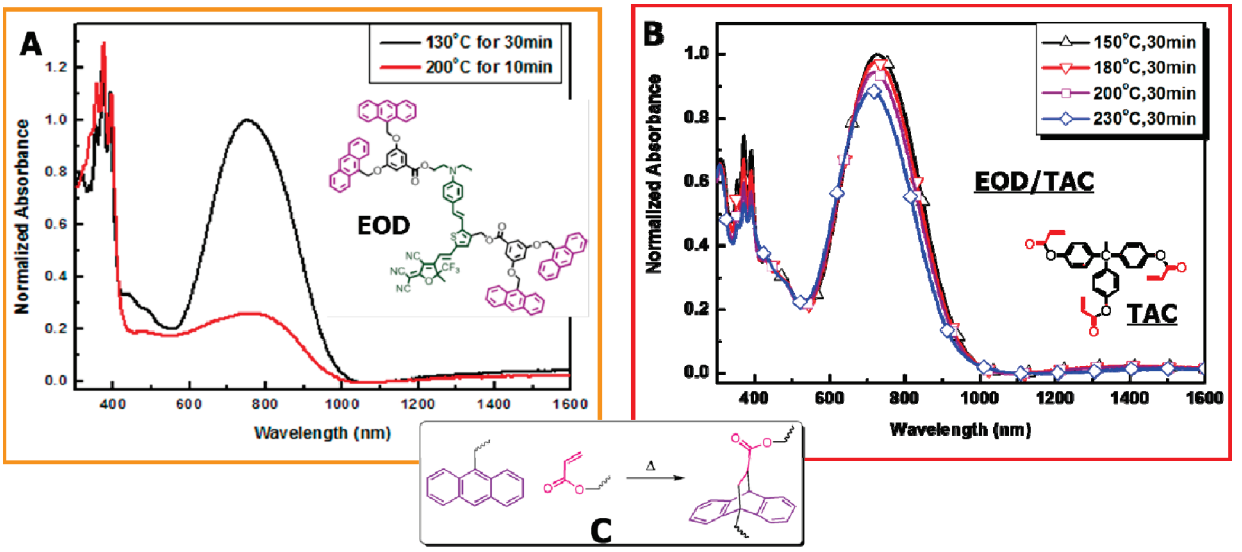

Figure 9. Thin film absorption spectra of (A) EOD only and (B) EOD/TAC upon thermal curing, and (C) the reaction protocol of anthracenyl and acrylate moieties.

chromophores could be well dispersed in the matrix at a relatively low temperature below T_g (stage A). At elevated temperatures, because of the large dipole moment and higher mobility of the molecules, the chromophores tend to pack with each other to form dimeric or oligomeric aggregates (stage B). This facilitates the bimolecular reaction through a tandem Diels−Alder (DA) and retro-DA reaction mechanism (stage C),[30] leading to the formation of degraded species with vanished NLO activities.

To address this problem, a reinforced site isolation strategy has been developed to separate large β dipolar chromophores apart for prolonging the stability and poling induced polar order of OEO materials through effective poling/lattice-hardening processes. As an example, a rigid dendritic chromophore EOD that was encapsulated with two anthracene-containing dendrons at the periphery was utilized as a model study (Figure 9). To evaluate the influence of reinforced site isolation on the thermal stability, a quantitative study was conducted by comparing the absorption spectra of thin films of EOD and EOD/TAC after isothermal heating at different curing temperatures. The EOD dendrimer can undergo a sequential cross-linking with TAC through the anthracene-acrylate-based DA cycloaddition, and the cured EOD/TAC is thermally stable up to 200−230 °C. In comparison, the thin film of single-component EOD experienced severe decomposition under the same isothermal heating conditions.

This reinforced site isolation approach has also been used to enhance thermal stability of EOD/TAC and its analogue series. The two rigid bulky anthracenyl dendrons provide fairly efficient site isolation to prevent intermolecular electrostatic interactions, whereas such site isolation can be preserved at higher temperature through sequential cross-linking. The resultant cross-linked dendrimers showed EO coefficients up to 84 pm/V at 1310 nm and exceptional long-term stability at 150 °C for more than 200 h. The poled films of EOD/TAC also passed the test of high temperature annealing, which were performed at 200 °C for 30 min. This strategy has been successfully applied to a variety of high T_g cross-linkable EO polymers with simplified material processing and fine-tuned reaction energetics and kinetics for cross-linking. Specifically, the bromo substitution on the anthracene moiety creates a significantly increased energy barrier for retro-DA reaction while having a relatively small effect on the DA activation energy barrier, leading to a more controllable temperature window for DA reaction and enhanced thermal stability (up to 300 °C) of the resultant cycloadducts. These materials exhibit both large r_{33} values (in the range of 70−120 pm/V) and excellent thermal stability (up to 250 °C), which are suitable candidates for photo-CMOS applications.[31]

5. Conclusions

Recent research and development of highly efficient OEO materials and their hybrid systems has enabled many significant advances in high-speed and broadband information technologies. Examples include the demonstration of low V_π and low loss EO modulators in hybrid polymer sol−gel waveguides, CMOS-compatible hybrid polymer silicon slotted waveguides, and EO polymer clad silicon nitride ring resonator modulators. These hybrid OEO systems provide a new paradigm of high bandwidth, small footprint, and low-energy consumption hybrid EO devices for telecom, datacom, and sensing applications.

Among all these demonstrations, several important issues related to more efficient poling and tailoring of material properties for specific applications in hybrid device systems have been discussed. The better understood conduction mechanism of OEO materials provides a useful guideline for improving material and device design to gain higher optical nonlinearities and low operating voltages. It is also of paramount importance to study the energy-level alignment between the interfaces of

OEO/electrode and the space-charge profile within the OEO/dielectric laminates. Meanwhile there are still remaining challenges to address the orientational polarization of OEO materials during the poling or self-assembly process because this is a transient process superimposed with space-charge responses.

The silicon OEO hybrid system is probably one of the most promising platforms that can be seamlessly integrated into silicon-based optoelectronic circuits. By using the best OEO materials available and scaling down the slot size of the silicon waveguides, further improvements in the device performance of hybrid OEO silicon slots can be expected in the near future. In this paradigm, slot waveguide-based modulators with V_π values of 10 mV or less should be possible, suggesting an improvement of nearly 2 orders of magnitude over current V_π values.[2]

Finally, the degree of non-centro-symmetric order observed in most of OEO materials is still below that of the maximum values predicted by theory. It is essential to explore new supramolecular engineering to further enhance polar order of poled or self-assembled OEO films. Innovative and generally applicable material processing need to be developed by taking all the lessons learned from the existing poled OEO materials and their hybrid systems.

An alternative route is to use the self-assembly or the layer-by-layer deposition process to create the polar order.[32] This is a viable approach over the sub-100 nm rail width of silicon slots, since the polar order of relatively thin EO materials can be achieved with less than 50 molecular layers. Such reduced device dimension suggests that surface initiated sequential synthesis can be automated, and potentially assisted by external electric fields. It must be conceded that current protocols used for the self-assembly of organic NLO materials, in particular layer-by-layer fabrication of extended polar lattices, are mainly based on dipolar chromophores with limited molecular hyperpolarizabilities. It also remains to be addressed about how to achieve a preferential orientation of chromophores within the slot that contains similar side-wall surfaces.

Acknowledgment. The authors thank all the current and previous members of the Jen research group for their contributions. Helpful discussions and technical assistance provided by Professors Robert Norwood, Nasser Peyghambarian (UA), Michael Hochberg, Antao Chen, Larry Dalton (UW), Michael Hayden (UMBC), Axel Scherer (Cal Tech), Ray Chen (UT), Manfred Eich (TUHH), William Steier (USC), Warren Herman (LPS), Yasufumi Enami (HU), and their colleagues are gratefully acknowledged. This work is supported by Office of Naval Research (ONR), National Science Foundation (NSF-STC program under DMR-0120967), the Defense Advanced Research Projects Agency (DARPA) MORPH program of supramolecular photonics, the Air Force office of Scientific Research (AFOSR), the World Class University (WCU) program through the National Research Foundation of Korea under the Ministry of Education, Science and Technology (R31-10035), Intel Corporation, and Boeing-Johnson Foundation.

References

(1) (a) Enami, Y.; DeRose, C. T.; Mathine, D.; Loychik, C.; Greenlee, C.; Norwood, R. A.; Kim, T. D.; Luo, J.; Tian, Y.; Jen, A. K.-Y.; Peyghambarian, N. *Nat. Photonics* **2007**, *1*, 183–185. (b) Hayden, M. *Nat. Photonics* **2007**, *1*, 138–139.

(2) (a) Hochberg, M.; Baehr-Jones, T.; Wang, G.; Shearn, M.; Harvard, K.; Luo, J.; Chen, B.; Shi, Z.; Lawson, R.; Sullivan, P.; Jen, A. K.-Y.; Dalton, L.; Scherer, A. *Nat. Mater.* **2006**, *5*, 703–709. (b) Baehr-Jones, T. W.; Hochberg, M. J. *J. Phys. Chem. C* **2008**, *112*, 8085–8090. (c) Baehr-Jones, T. W.; Hochberg, M. J. *Nat. Photonics* **2009**, *3*, 193–194. (d) Reed, G. T.; Mashanovich, G.; Gardes, F. Y.; Thomson, D. J. *Nat. Photonics* **2010**, *4*, 518–526.

(3) (a) Koos, C.; Vorreau, P.; Vallaitis, T.; Dumon, P.; Bogaerts, W.; Baets, R.; Esembeson, B.; Biaggio, I.; Michinobu, T.; Diederich, F.; Freude, W.; Leuthold, J. *Nat. Photonics* **2009**, *3*, 216–219. (b) Leuthold, J.; Freude, W.; Brosi, J.-M.; Baets, R.; Dumon, P.; Biaggio, I.; Scimeca, M. L.; Diederich, F.; Frank, B.; Koos, C. *Proc. IEEE* **2009**, *97*, 1304–1316. (c) Leuthold, J.; Koos, C.; Freude, W. *Nat. Photonics* **2010**, *4*, 535–544.

(4) (a) Cho, M. J.; Choi, D. H.; Sullivan, P. A.; Akelaitis, A. J. P.; Dalton, L. R. *Prog. Polym. Sci.* **2008**, *33*, 1013–1058. (b) Luo, J.; Zhou, X.; Jen, A. K.-Y. *J. Mater. Chem.* **2009**, *19*, 7410–7424. (c) Dalton, L. R.; Sullivan, P. A.; Bale, D. H. *Chem. Rev.* **2010**, *110*, 25–55. (d) Verbiest, T.; Houbrechts, S.; Kauranen, M.; Clays, K.; Persoons, A. *J. Mater. Chem.* **1997**, *7*, 2175–2189. (e) Kajzar, F.; Lee, K. S.; Jen, A. K-Y. *Adv. Polym. Sci.* **2003**, *161*, 1–85. (f) Burland, D. M.; Miller, R. D.; Walsh, C. A. *Chem. Rev.* **1994**, *94*, 31–75. (g) Marks, T. J.; Ratner, M. A. *Angew. Chem., Int. Ed.* **1995**, *34*, 155–173. (h) Marder, S. R.; Kippeien, B.; Jen, A. K.-Y.; Peyghambarian, N. *Nature* **1997**, *388*, 845–851.

(5) (a) Sprave, M.; Blum, R.; Eich, M. *Appl. Phys. Lett.* **1996**, *69*, 2962–2964. (b) Blum, R.; Sprave, M.; Sablotny, J.; Eich, M. *J. Opt. Soc. Am. B: Opt. Phys.* **1998**, *15*, 318–328.

(6) Drummond, J. P.; Clarson, S. J.; Zetts, J. S.; Hopkins, F. K.; Carraci, S. J. *Appl. Phys. Lett.* **1999**, *14*, 368–370.

(7) Grote, J. G.; Zetts, J. S.; Nelson, R. L.; Hopkins, F. K.; Dalton, L. R.; Zhang, C.; Steier, W. H. *Opt. Eng.* **2001**, *40*, 2464–2473.

(8) DeRose, C. T.; Enami, Y.; Loychik, C.; Norwood, R. A.; Mathine, D.; Fallahi, M.; Peyghambarian, N.; Luo, J. D.; Jen, A. K.-Y.; Kathaperumal, M.; Yamamoto, M. *Appl. Phys. Lett.* **2006**, *89*, 131102/1–131102/3.

(9) (a) Norwood, R. A.; Derose, C.; Enami, Y.; Gan, H.; Greenlee, C.; Himmelhuber, R.; Kropachev, O.; Loychik, C.; Mathine, D.; Merzylak, Y.; Fallahi, M.; Peyghambarian, N. *J. Nonlinear Opt. Phys. Mater.* **2007**, *16*, 217–230. (b) Montanari, G. C.; Morshuis, P. H. F. *IEEE Trans. Dielectr. Electr. Insul.* **2005**, *12*, 754–767.

(10) Enami, Y.; Mathine, D.; DeRose, C. T.; Norwood, R. A.; Luo, J.; Jen, A. K.-Y.; Peyghambarian, N. *Appl. Phys. Lett.* **2007**, *91*, 093505/1–093505/3.

(11) DeRose, C. T.; Himmelhuber, R.; Mathine, D.; Norwood, R. A.; Luo, J.; Jen, A. K.-Y.; Peyghambarian, N. *Opt. Exp.* **2009**, *17*, 3316–3321.

(12) Huang, S.; Kim, T.-D.; Luo, J.; Hau, S. K.; Shi, Z.; Zhou, X.-H.; Yip, H.-L.; Jen, A. K.-Y. *Appl. Phys. Lett.* **2010**, *96*, 243311/1–243311/3.

(13) (a) Kim, T.-D.; Luo, J.; Cheng, Y.-J.; Shi, Z.; Hau, S.; Jang, S.-H.; Zhou, X.-H.; Tian, Y.; Polishak, B.; Huang, S.; Ma, H.; Dalton, L. R.; Jen, A. K.-Y. *J. Phys. Chem. C* **2008**, *112*, 8091–8098. (b) Cheng, Y.-J.; Luo, J.; Huang, S.; Zhou, X.; Shi, Z.; Kim, T.-D.; Bale, D. H.; Takahashi, S.; Yick, A.; Polishak, B. M.; Jang, S.-H.; Dalton, L. R.; R., P. J.; Steier, W. H.; Jen, A. K.-Y. *Chem. Mater.* **2008**, *20*, 5047–5054.

(14) Gratzel, M. *Nature* **2001**, *414*, 338–344.

(15) (a) Arkhipov, V. I.; Emelianova, E. V.; Tak, Y. H.; Bassler, H. *J. Appl. Phys.* **1998**, *84*, 848–856. (b) Wolf, U.; Arkhipov, V. I.; Bassler, H. *Phys. Rev. B* **1999**, *59*, 7507–7513. (c) Arkhipov, V. I.; Wolf, U.; Bassler, H. *Phys. Rev. B* **1999**, *59*, 7514–7520. (d) Arkhipov, V. I.; von Seggern, H.; Emelianova, E. V. *Appl. Phys. Lett.* **2003**, *83*, 5074–5076.

(16) Baehr-Jones, T.; Hochberg, M.; Wang, G.; Lawson, R.; Liao, Y.; Sullivan, P. A.; Dalton, L.; Jen, A. K.-Y.; Scherer, A. *Opt. Exp.* **2005**, *13*, 5216–5226.

(17) Baehr-Jones, T.; Penkov, B.; Huang, J.; Sullivan, P.; Davies, J.; Takayesu, J.; Luo, J.; Kim, T.-D.; Dalton, L.; Jen, A.; Hochberg, M.; Scherer, A. *Appl. Phys. Lett.* **2008**, *92*, 163303/1–163303/3.

(18) Wülbern, J. H.; Hampe, J.; Petrov, A.; Eich, M.; Luo, J.; Jen, A. K.-Y.; Di Falco, A.; Krauss, T. F.; Bruns, J. *Appl. Phys. Lett.* **2009**, *94*, 241107/1–241107/3.

(19) Wülbern, J. H.; Prorok, S.; Hampe, J.; Petrov, A.; Eich, M.; Luo, J.; Jen, A. K.-Y.; Jenett, M.; Jacob, A. *Opt. Lett.* **2010**, *35*, 2753–2755.

(20) (a) Lin, C.-Y.; Lee, B.; Wang, A. X.; Lai, W.-C.; Chakravarty, S.; Liu, Y.; Kwong, D.; Chen, R. T.; Luo, J.; Jen, A. K. Y. *Proc. SPIE* **2010**, *7607*, 76070D/1–76070D/8. (b) Lin, C.-Y.; Wang, X.; Chakravarty, S.; Lee, B.; Lai, W.-C.; Luo, J.; Jen, A. K. Y.; Chen, R. T. *Appl. Phys. Lett.* **2010**, *97*, 093304/1–093304/3.

(21) Wang, X.; Lin, C.-Y.; Chakravarty, S.; Luo, J.; Jen, A. K. Y.; Chen, R. T. **2010**, manuscript submitted.

(22) Ding, R.; Baehr-Jones, T.; Liu, Y.; Bojko, R.; Witzens, J.; Huang, S.; Luo, J.; Benight, S.; Sullivan, P.; Fedeli, J-M; Fournier, M.; Dalton, L.; Jen, A.; Hochberg, M. *Opt. Exp.* **2010**, *18*, 15618–15623.

(23) (a) Zheng, Y.; Wee, A. T. S.; Troadec, C.; Chandrasekhar, N. *Appl. Phys. Lett.* **2009**, *95*, 143303/1–143303/3. (b) Agrawal, R.; Kumar, P.;

Ghosh, S.; Mahapatro, A. K. *Appl. Phys. Lett.* **2008**, *93*, 073311/1–073311/3. (c) Baranovskii, S. D.; Rubel, O.; Jansson, F.; Oesterbacka, R. *Adv. Polym. Sci.* **2010**, *223*, 45–71.

(24) (a) Alasaarela, T.; Säynätjoki, A.; Hakkarainen, T.; Honkanen, S. *Opt. Eng. Lett.* **2009**, *48*, 080502−1–080502−3. (b) Säynätjoki, A.; Alasaarela, T.; Khanna, A.; Karvonen, L.; Stenberg, P.; Kuittinen, M.; Tervonen, A.; Honkanen, S. *Opt. Exp.* **2009**, *17*, 21066–21076.

(25) (a) Mohammed, E.; Alduino, A.; Thomas, T.; Braunisch, H.; Lu, D.; Heck, J.; Liu, A.; Young, I.; Barnett, B.; Vandentop, G.; Mooney, R. *Intel Technol. J.* **2004**, *8*, 115–127. (b) Kobrinsky, M. J.; Zheng, J. F.; Barnett, B. C.; Mohammed, E.; Reshotko, M.; Roberston, F.; List, S.; Young, I.; Cadien, K. *Intel Technol. J.* **2004**, *8*, 129–141. (c) Young, I. A.; Mohammed, E.; Liao, J. T. S.; Kern, A. M.; Palermo, S.; Block, B. A.; Reshotko, M. R.; Chang, P. L. D. *IEEE J. Solid-State Circuits* **2010**, *45*, 235–248.

(26) Block, B. A.; Younkin1, T. R.; Davids, P. S.; Reshotko, M. R.; Chang, P.; Polishak, B.; Huang, S.; Luo, J; Jen, A. K.-Y. *Opt. Express* **2008**, *16*, 18326–18333.

(27) Block B.; Liff, S.; Chang, P., private communications.

(28) (a) Luo, J.; Liu, S.; Haller, M.; Liu, L.; Ma, H.; Jen, A. K.-Y. *Adv. Mater.* **2002**, *14*, 1763–1768. (b) Shi, Z.; Luo, J.; Huang, S.; Cheng, Y,-J.; Kim, T.-D.; Polishak, B.; Zhou, X.-H.; Tian, Y.; Jang, S.-H.; Daniel, K.; Overney, R.; Youkin, T.; Jen, A. K-Y. *Macromolecules* **2009**, *42*, 2438–2445.

(29) (a) Chen, T.-A.; Jen, A. K.-Y.; Cai, Y. *J. Am. Chem. Soc.* **1995**, *117*, 7295–7296. (b) Miller, R. D.; Burland, D. M.; Jurich, M.; Lee, V. Y.; Moylan, C. R.; Thackara, J. I.; Twieg, R. J.; Verbiest, T.; Volksen, W. *Macromolecules* **1995**, *28*, 4970–4974.

(30) Shi, Z.; Luo, J.; Huang, S.; Zhou, X.-H.; Kim, T.-D.; Cheng, Y.-J.; Polishak, B.; Youkin, T.; Block, B.; Jen, A. K.-Y. *Chem. Mater.* **2008**, *20*, 6372–6377.

(31) Shi, Z; Liang, W; Huang, S.; Luo, J.; Polishak, B. M.; Li, X.; Younkin, T. R.; Block, B. A.; Jen, A. K.-Y. *Chem. Mater.* **2010**, *22*, 5601–5608.

(32) (a) Zhu, P.; Kang, H.; Facchetti, A.; Evmenenko, G.; Dutta, P.; Marks, T. J. *J. Am. Chem. Soc.* **2003**, *125*, 11496–11497. (b) Facchetti, A.; Abbotto, A.; Beverina, L.; van der Boom, M. E.; Dutta, P.; Evmenenko, G.; Pagani, G. A.; Marks, T. J. *Chem. Mater.* **2003**, *15*, 1064–1072. (c) Facchetti, A.; Annoni, E.; Beverina, L.; Morone, M.; Zhu, P.; Marks, T. J.; Pagani, G. A. *Nat. Mater.* **2004**, *3*, 910–917. (d) Frattarelli, D.; Schiavo, M.; Facchetti, A.; Ratner, M. A.; Marks, T. J. *J. Am. Chem. Soc.* **2009**, *131*, 12595–12612. (e) Roberts, M. J.; Lindsay, G. A.; Herman, W. N.; Wynne, K. J. *J. Am. Chem. Soc.* **1998**, *120*, 11202–11203. (f) Cai, C.; Muller, B.; Weckesser, J.; Barth, J. V.; Tao, Y.; Bosch, M. M.; Kundig, A.; Bosshard, C.; Biaggio, I.; Gunter, P. *Adv. Mater.* **1999**, *11*, 750–754. (g) Khan, R. U. A.; Kwon, O.-P.; Tapponnier, A.; Rashid, A. N.; Gunter, P. *Adv. Funct. Mater.* **2006**, *16*, 180–188.